PTV APPLICATION TO THE STUDY OF INTERNAL WAVES GENERATED BY PENETRATIVE CONVECTION

A. Cenedese[a] - G. Mancini[a]

[a] Department of Hydraulics, Transportation and Roads, University of Rome "La Sapienza"
Via Eudossiana 18, 00184 Rome, Italy
Phone: +39 06 44585033
+39 06 44585217
E-mail giu@dits.ing.uniroma1.it

Abstract

A laboratory experiment was performed to simulate *penetrative convection* in a stratified lake. Penetrative convection concerns the advance of a turbulent fluid into a fluid layer of stable stratification. This phenomenon is commonly observed in lakes when, owing to surface nocturnal cooling or to superficial wave breaking the initially stable environment near to the free surface is affected by convection with the advancing instable layer showing several domes which penetrate small distances into the stable layer. Water quality in lakes is highly dependent on entrainment of nutrients and pollutants from the deeper hypolimnium (Denman, 1995). Entrainment in a stratified lake may be dominated by thermal convection, organized coherent structures ("large eddies"), or internal waves. The excitation of gravity waves in a stratified lake is important for several reason. Waves can propagate downward through the stratified metalimniom of the lake producing entrainment in the upper layer (figure 1 and 2), interact with other long wave excited by wind, with patches of turbulence (Weinstock, 1984), can be reflected and create an oscillating boundary layer at the bottom of the lake with the consequent raising of settled matter (Stevens, 1994). A number of laboratory and theoretical models have been developed for internal wave propagation in stratified fluids. However the complex role of internal waves in lake dynamic is still not well understood from a fundamental point of view. It was the aim of this paper to study internal waves generated by thermal impact on the interface during penetrative convection. Particle Tracking Velocimetry (PTV) was employed to reconstruct the field of motion. Specifically this technique allows the lagrangian tracking of tracer particles placed in the fluid. The simulation features, with a growing thickness of mixed layer (ML) depth and a continuous decrease of heat flux at the surface, make not possible to consider the analyzed system in a steady state. However, the time scale of the studied convective phenomena is definitively smaller than the time for significant changes in ML mean temperature and depth. The vertical structure of potential temperature during the deepening of the mixed layer was analyzed and related to the vertical and horizontal velocity as obtained by PTV techniques. The results confirmed the effectiveness of the employed tracking technique to study the internal wave field. Spectral analysis of temperature and velocity signals highlighted the presence of several frequency where energy is concentrated, with the most important one corresponding to the initial strongest temperature jump. An interesting result was the enhanced increase of temperature caused by internal wave in the metalimnion. As the deeper colder fluid is raised up by internal wave oscillation it becomes surrounded by lighter fluid. Without loosing its identity the colder fluid is able to increase its temperature by thermal diffusion acquiring the heat of the hotter fluid. The result is a heat transfer rate much higher than the one due to simple molecular diffusion because of the enhanced temperature difference of the two fluid masses. The same happens to any other substance whose concentration presents a vertical gradient.

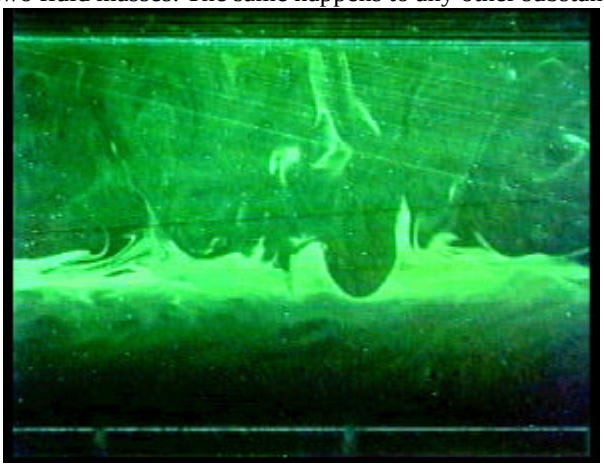

Figure 1. LIF visualization of the impact of a convective eddy on the interface

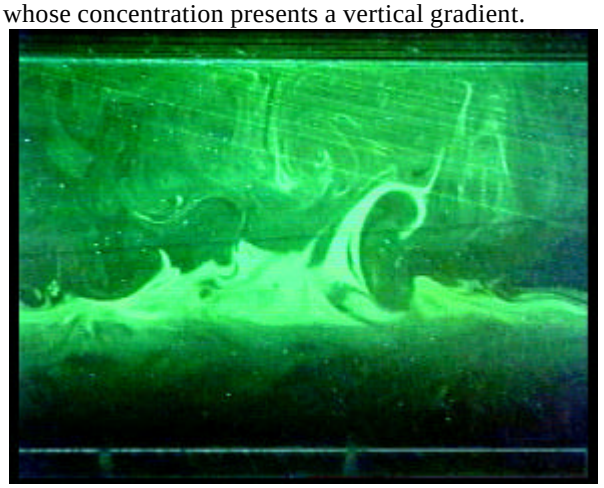

Figure 2. LIF visualization of the rise of heavier fluid inside the mixed layer

Introduction.

Models of the structure of stratified oceans and lakes use bulk parameters to predict a variety of processes that control the ecology of natural systems. The success of such approach in predicting even smaller scale phenomena has not a parallel in modeling turbulent properties. Particularly the interaction of convective turbulence and the density interface is not well understood. Analytic solutions for such turbulent motion are not available and there appears to be little hope of finding such solutions in the near future. Measurements by (Ivey, 1989) indicate that in and below the main thermocline, turbulence occurs in patches. Field data in lakes and in the oceans suggest, at least in the stratified metalimnion, the water offers very low internal vertical exchange for both momentum and mass, with the coefficients close to the molecular value. The momentum transport which takes place in this layer is dominated by internal wave transport, therefore, the adoption of complicated closure schemes based on shear turbulence which neglect internal waves is of questionable value. The vertical transport albeit small, is however crucial from a biological point of view as it nourishes the plankton in the surface layer with nutrients contained in the deeper water. Hannoun *et* al. (1988) showed that even if internal waves interact in a weakly way, so not to break into turbulence, such interactions may result in a dispersive motion in the horizontal plane. This motion can be important for redistributing nutrients and particles even when the fluid is not fully turbulent. The presence of a stable stratification beneath the thermocline is significant in that internal waves generated by the response of the thermocline to the motions in the turbulent mixed layer can drain away a fraction of the energy of the mixed layer. In most of the models, the transfer of energy from a turbulent ocean or lake surface mixing layer to the deeper, relatively quiescent, fluid beneath is currently either ignored or assumed to be a fixed proportion of the turbulent kinetic energy in the surface layer. The majority of introduced energy in the experiments on this topic is lost to viscosity without playing a role in the increase in potential or kinetic energy of the system (Andreasson, 1992). However, while energy loss through the base of the surface mixed layer might represent only a small portion of the energy budget, it may be significant when compared to the energy transferred to potential energy through entrainment or to existing kinetic energy levels beneath the surface. Linden (1975) found that the rate of increase of potential energy of a water column produced by the penetration of a turbulent layer into a region of constant density gradient is proportional to the rate of input of kinetic energy by the turbulent motions at the bottom of the mixed layer. This phenomenon can, in turn, decrease the rate of entrainment of the stable fluid inside the mixed layer. When, such as in the case of penetrative convection, there is no mean shear, a much reduced rate of deepening is produced. Consequently it appears that the presence of a mean shear allows a larger, and indeed constant fraction of the surface energy to be transmitted to the interface. Stull (1976) found that the amount of energy carried vertically away from the mixed layer by the internal gravity waves is small for strong thermocline. However, when the density jump is weak and the turbulent/convective mixing in the boundary layer is vigorous, a significant fraction of the energy of the overshooting elements can be lost. Linden (1975) Studied mixing induced by impinging spherical vortex rings of characteristic length and velocity scales, l and u respectively, on a sharp density interface. Upon impact, both the interface and the rings distort, and when the maximum deflection is reached, the buoyancy forces cause the interface to recoil and splash heavy fluid into the upper layer. Comparing the maximum possible vertical energy flux per unit horizontal area, carried by the waves, with the observed rate of change of potential energy of a fluid column of unit horizontal area, Linden found up to 50% reduction in the mixing rate due to the presence of internal waves. Dahm et al (1989) found that at large Richardson Number Ri the eddies tend to flatten at the interface as if they were colliding on a rigid surface. Measurements of the characteristic horizontal length scale of the distorted eddies suggest that eddy flattening is effective when $Ri > 15$ or so. Dahm et al (1989) also observed that the dominant mechanism at large Ri is interfacial wave breaking which causes spatially and temporally intermittent mixed patches to develop and merge with the mixed layer. Under these conditions only the large scale are affected by the interface while the small scales remain isotropic. Most of the kinetic energy of the impinging eddies is used to raise heavy fluid out of the interface and thus the rate of change of potential energy can be considered to be proportional to the divergence of the kinetic energy flux. According to Long (1978) at high Ri the eddies simply flatten at the interface causing an intercomponent energy transfer from the vertical to horizontal components.

In the present experiment the deepening of a convective mixed layer in a stratified lake was simulated. LIF visualization, temperature measures and velocity measures by means of PTV, were employed to examine the effect of convective-driven perturbation at the base of the mixed layer under conditions where there is no vertical share.

Experimental setup and procedure

The experiments were conducted in a tank with glass sidewalls of dimension 40 x 40 x 41 cm in the two horizontal and vertical directions respectively. The tank was filled with fresh water at a temperature of 21.6 °C till a depth of 40 cm, and cooled from above by a heat exchanger controlled by a cryostat. With reference to figure 3, in which a sketch of the experimental apparatus is represented The countercurrent shell and tube exchanger consisted of bars of

1 cm^2 in cross section, equally spaced by 2 cm to maintain the free surface condition. This choice did not allow a direct measure of the heat flux at the surface. The stratification was obtained by first lowering the heat exchanger to a depth of 7 cm and allowing hot water into it. After the water above the heat exchanger reached the desired temperature (8 °C hotter than the water below) the heat exchanger was carefully lowered by 3 cm to erode the temperature gradient beneath it and thus sharpen the interface between the two layers. Finally the heat exchanger was raised to the water surface, emptied and filled with water at the same temperature of the lower layer. The final result was a sharp interface between 10 and 15 cm depth. Cooling was then applied at the top of the tank and the upper layer became convective.

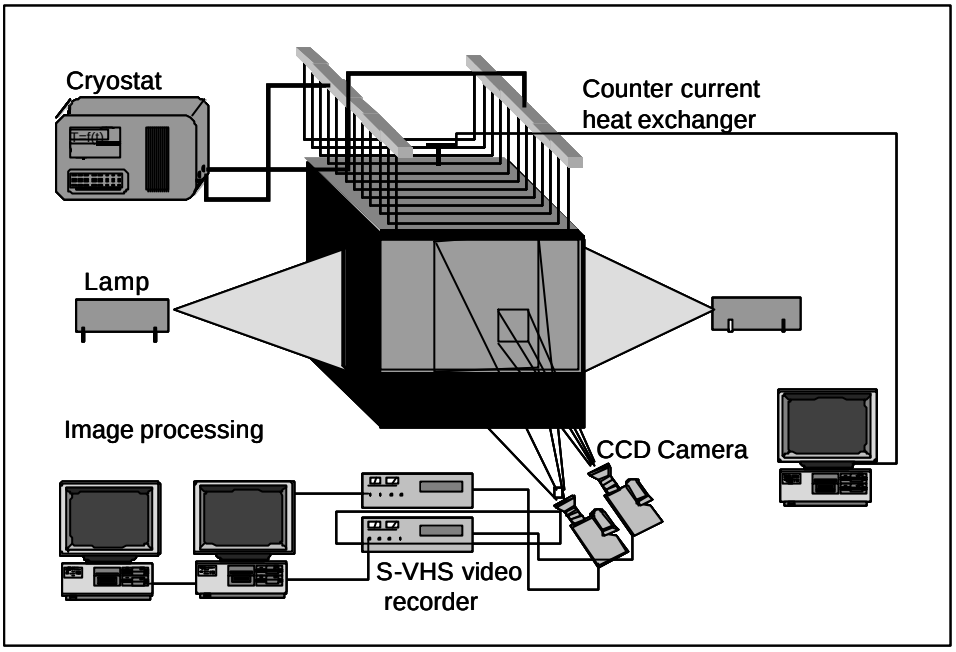

Figure 3 Experimental set up

The two velocity components, on a vertical plane, were measured by gathering a time-sequence of images. Two facing 500 W lamps continuously illuminated the tank through a slot, generating a 2 cm thick light sheet positioned at 2/3 of the width of the tank. The fluid was seeded with small pollen particles, 50 μm in mean diameter. Two video cameras (shutter 1/25 s), orthogonal to the light sheet, framed series of images which were stored on two tapes by an S-VHS video-recorder, and a common VHS recorder.

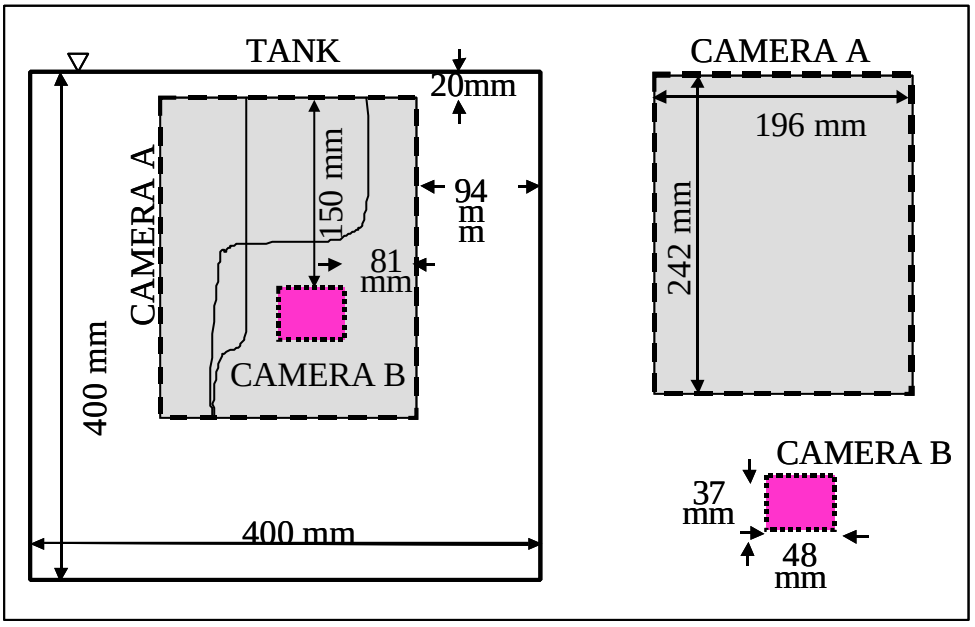

Figure 4. Dimensions and relative positions of the two framed areas.

The first video camera (video camera A) framed an image of 2/3 of the entire depth of the tank (24 cm depth by 20 cm width), so including epilimnion, metalimnion and part of the hypolomnion. The second video camera (video camera B) framed a smaller area of 4 cm depth by 5 cm width, focusing on the entrainment zone inside the metalimnion. Particle trajectories were determined by assuming that the displacement of the barycentre of the particle, between two successive frames, was less than a given parameter *D*, and that the shifting of the real trajectory from a theoretical linear one, at the third frame, was lesser than a second parameter *e* (figure 5).

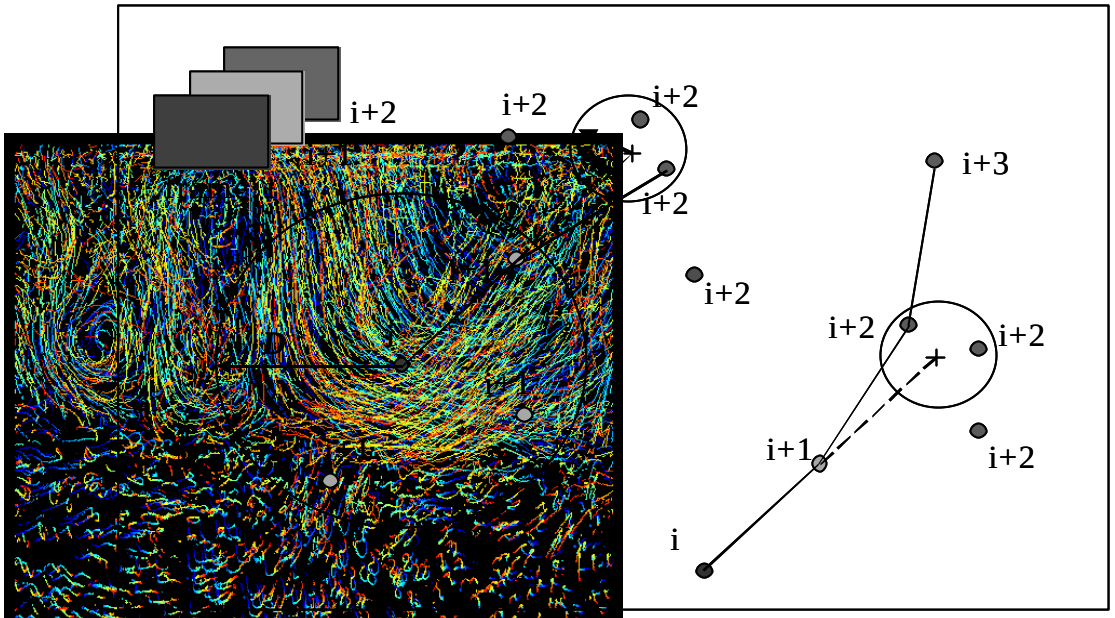

ocimetry technique

ty and maximum acceleration assumed for the particle
rajectories is preceded by the continuation of the existing
d breaking the trajectories in several small pieces. The
ough a sensitivity analysis.

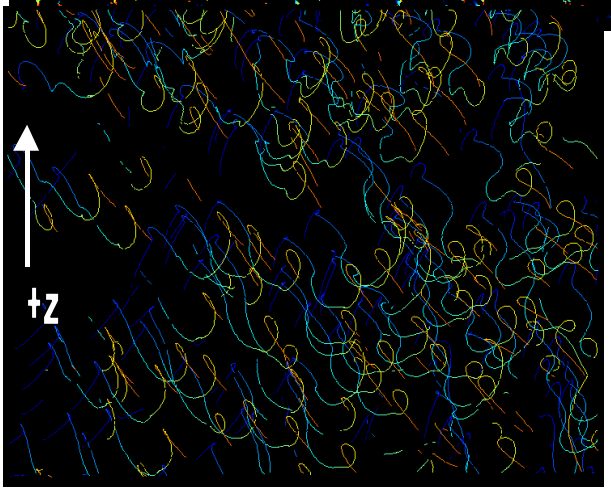

Figure 7 Trajectories reconstruction from camera B

Figure 6 Trajectories reconstruction from camera A

About 1200 particle barycentres and 600-800 trajectories were validated on each video frame for video camera A (figure 6), while about 100 particle barycentres and an equal number of trajectories were validated on each frame of video camera B (figure 7). During the image acquisition, 6 thermocouples, located at different depths in the tank, acquired the time history of the temperature. Four temperature profiles were measured in the middle of the tank by a mobile thermocouple, with a spatial resolution along the vertical direction of 0.5 cm.

Experimental results

Temperature and Buoyancy frequency profiles

A series of temperature-depth profiles is shown on figure 8. Each profile was obtained by averaging over 240 s of the measurements of the different thermocouples because of the low resolution of thermocouple signals but, above all, to the random presence of descending thermals close to the probes that made the instantaneous temperature profile not representative of mixed layer mean temperature profile.

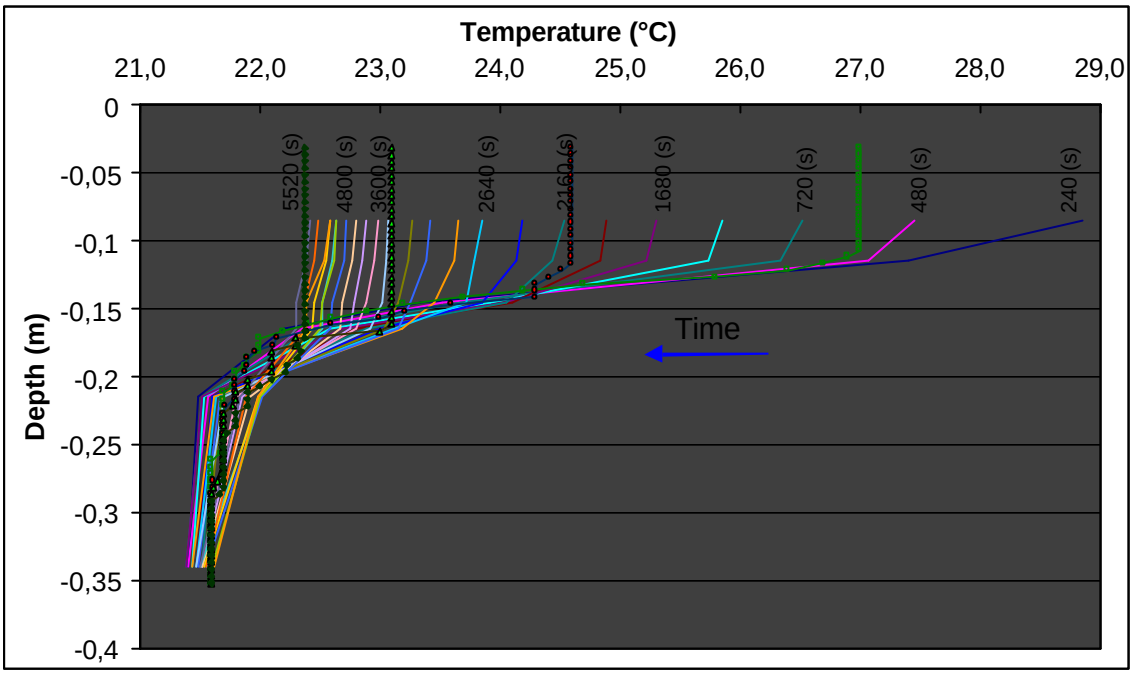

Figure 8 Variation of Temperature at different depths versus time. The bold profiles are those measured by means of the mobile thermocouple.

It is seen that all the profiles show two layers separated by a growing region of temperature gradient. At the upper edge of this region the temperature gradient goes sharply to zero, according to the well mixed condition of the upper layer. (it is worth pointing out that the uniformity of mean temperature over the depth of the mixed layer was verified in details by arranging all the thermocouples inside the mixed layer in a previous experiment, then tested during the current experiments by means of the mobile thermocouple).

On the basis of these results, only one of the six thermocouples was located inside the mixed layer. The 2nd, 3rd and 4th thermocouples were located in the strongly stratified zone simulating the metalimnion. Beyond these depths the temperature was again much more uniform and two thermocouples were sufficient to cover the remaining depth. The temperature gradient decreases over the time due to the combined effects of mixed layer cooling and entrainment of colder fluid from the lower layer. Figure 9 shows the time series of temperature measurements as detected by the six thermocouples. Clearly visible is the diversity of the temperature inside the mixed layer and the temperatures in the metalimnion as the interface approaches. Also it is evident the time the single thermocouple enter the mixed layer. The frequency of the oscillations varies as well as the amplitude of the fluctuations at the different frequencies and this heaving was the result of internal wave activity. Particularly interesting it is the fast increase in temperature registered by thermocouples closer to the interface. The enhanced heating up is due to the exchange of heat between fluid masses, originally at different depths (and so different temperatures), which periodically become closer because of to the oscillations induced by internal waves. The deepening of the mixed layer is evident from the observation of temperature profiles but the low spatial resolution of the few thermocouples

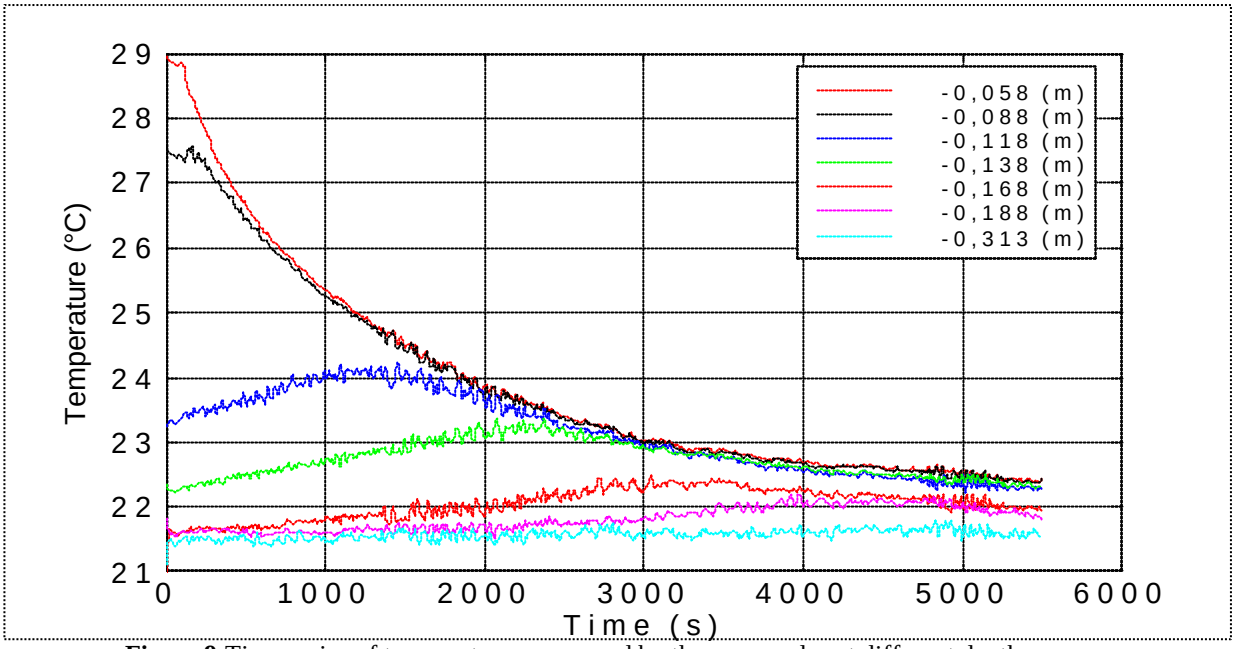

Figure 9 Time series of temperatures measured by thermocouples at different depths

prevented to obtain the mixed layer deepening law by means of temperature measurements. However this law was obtained by the vertical velocity variance profiles (Cenedese et Mancini, 1999).

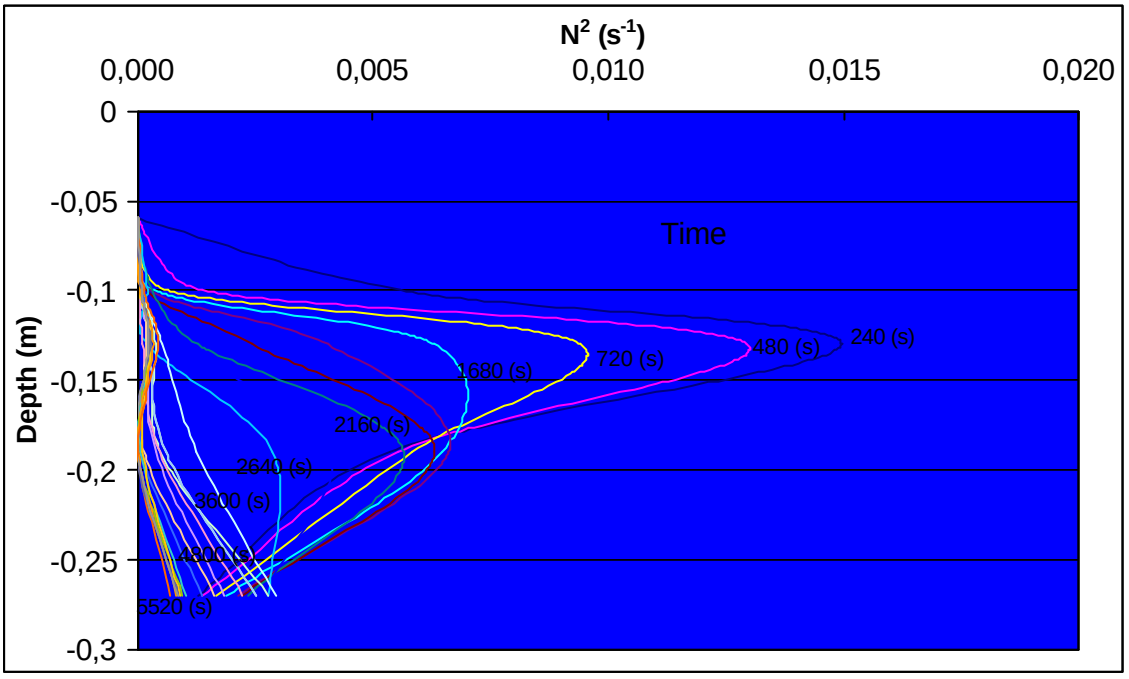

Figure 10 Buoyancy frequency profiles over the time

Figure 10 shows the buoyancy frequency profiles as obtained from the temperature profiles. The buoyancy frequency N (Brunt Vaisäla frequency) represents the upper limit of frequency for which wave motions can exists in a stratified fluid and it is defined by:

$$N = \left(-\frac{g}{r_0} \frac{\partial r}{\partial z} \right)^{1/2} \qquad (1)$$

where ρ is the density at depth z , ρ_0 is the density of the water at the mean temperature and g is the gravity acceleration. In a fluid with variable N waves will be trapped within the layer where N exceeds the imposed frequency. However sharp interfaces can sustain waves of arbitrary frequency. As the temperature profile evolves over the time of the experiment so the buoyancy frequency profile does, varying the direction of propagation of the waves and the amount of energy transfered to the deeper layer through internal waves activity. The frequency content of the temperature signals is best seen by plotting the power spectral density and an example for the temperature at 20 cm (in the middle of metalimnion) is shown in figure 11. The spectrum decreases fairly rapid from the minimum frequency to a frequency of about $10^{-2.5}$ (320 seconds). The energy in this bandwidth arises mainly from long waves fluctuations. Beyond this frequency band there is a bandwidth where the energy show few peaks last of whom at a frequency of about $10^{-1,819}$ Hz (around 66 seconds) which corresponds to the largest (0,152 Hz). The energy in this regions appears to come from free internal waves which are propagating randomly throughout the stratified layer (metalimnion) which serves as a wave guide. These waves are energized by either wave-wave interaction or directly established by turbulent events in the surface layer or internally in the metalimnion itself.

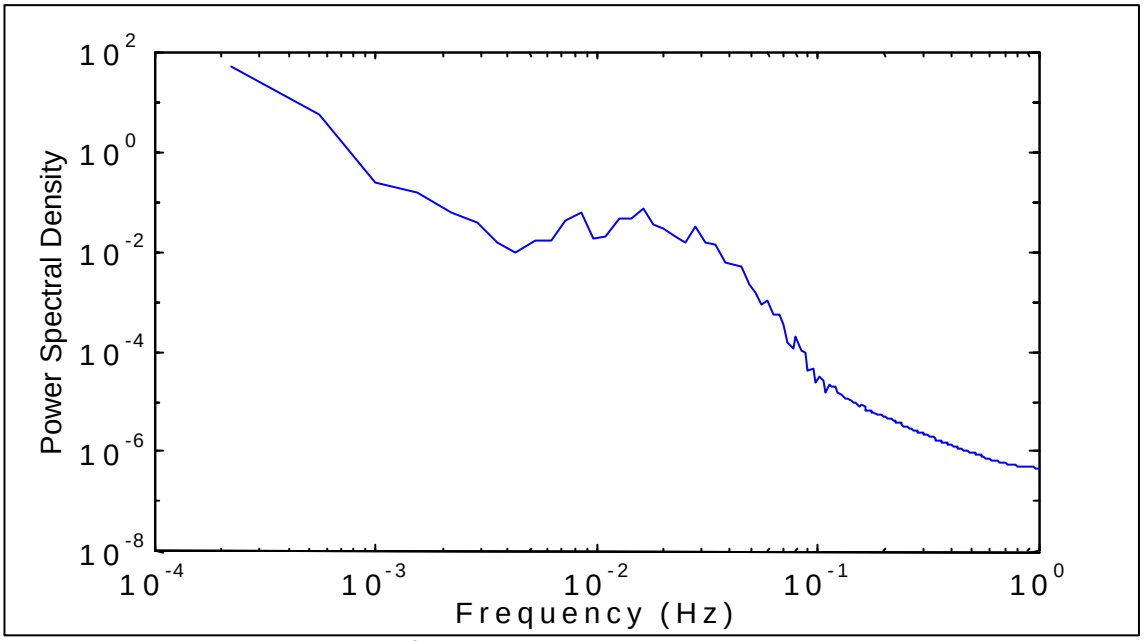

Figure 11 Power spectral density of the temperature at the depth -0.188 m

Most of the energy is contained in eddies, non symmetric waves and, at high frequency, very strongly non-linear waves. Beyond the buoyancy cut off the energy is seen to decrease rapidly again. The convective instabilities in the mixed layer interacts with the internal wave field to transfer the energy to motions of decreasing scale. The turbulent motions absorbs some of this energy and transfers it to even smaller scale where ultimately it is dissipated in the form of heat and used to ad just the potential energy of the system through the buoyancy flux.

Velocity profiles and internal wave field

The velocity field on a regular grid was obtained by inverse distance interpolation (figure 13). As a result, two components of the velocity were known on a grid with 30 cells along the horizontal and 39 along the vertical for video camera A at 4.17 Hz rate. Results were averaged over 24 images, (0.96 s), which is small compared to the time scale *T* of the phenomenon (40 s). The total acquisition time was about 140 *T* (1.5 hrs).

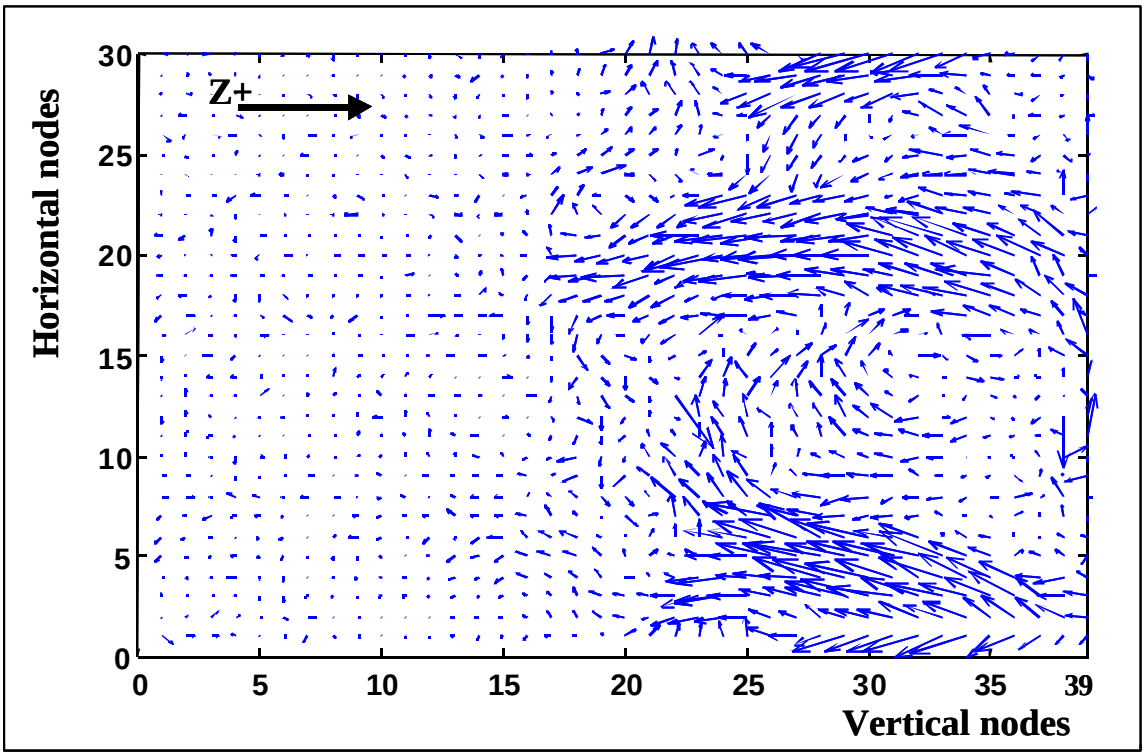

Figura 13 Eulerian velocity field over a regular grid of 30 rows (horizontal) by 39 columns (vertical). Cell dimension is about 0.0065 m.) Figure is rotated by 90° clockwise so that the free surface is on the right side)

Vertical and horizontal velocity components at different depths vs time, as obtained by the image of camera A, are plotted in figure 14 and 15 respectively. The different equidistant positions of the plotted velocities over the vertical range from the free surface to the end of metalimnion. It is easily recognizable the growth of the mixed layer whose lower boundary progressively reaches the "quiescent" lower layers, stirring them and producing entrainment.
The velocity behavior of the layers underneath the interface points out the presence of the internal wave field with fluid particles moving in paths with amplitude decreasing with distance from the interface. Much more difficult it is to identify a peculiar period for the thermals. This is due two conditions: first of all, thermals grows at unpredictable position of the free surface due to local concentration of energy (i.e. instability); seconds the light sheet is only 2 centimeters thick to avoid tracking errors. It means that only vertical sections of the three dimensional structures can be framed by the camera, causing identification troubles.
Vertical velocity component as obtained by the image of camera B is shown in figure 16. It is evident the effect of the interface approach with the increasing oscillations till the velocity assumes the mixed layer values as the interface passes by. Image analysis showed how turbulent/convective elements from the base of the mixed layer overshoot short distances downward into the stable region and then raise back into the turbulent layer. The following collapse is accompanied by a great deal of three dimensional, smaller-scale motion. These small scale motions are needed to promote permanent mixing but are apparently only partially effective as the free convection allows much

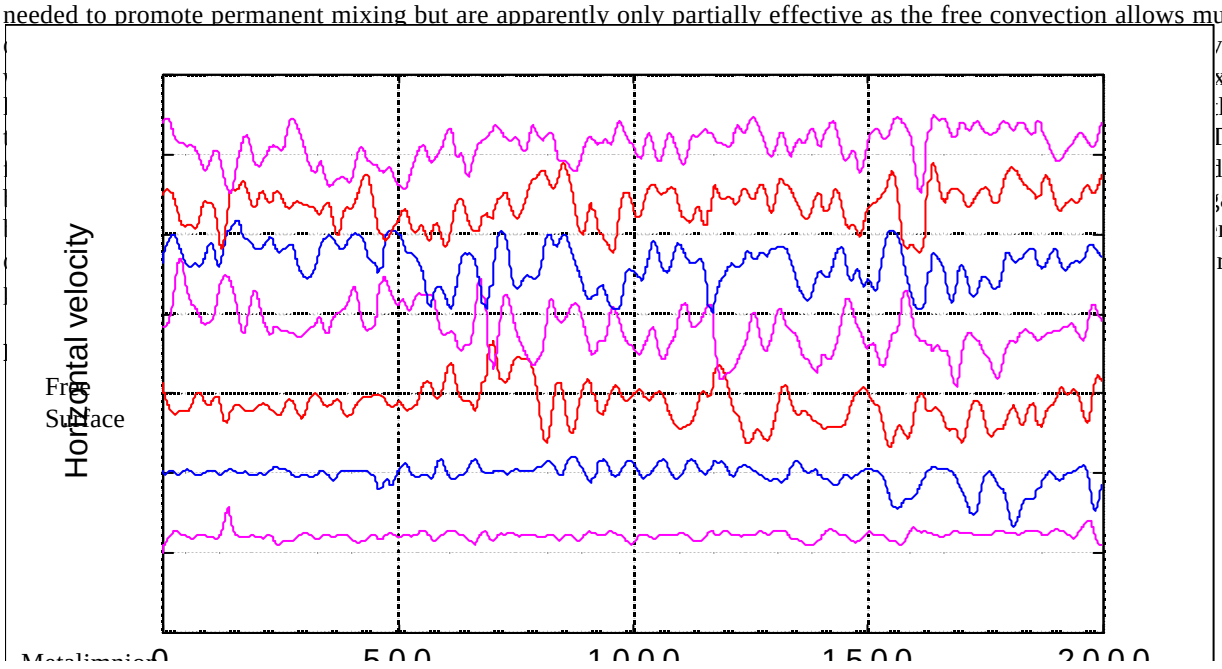

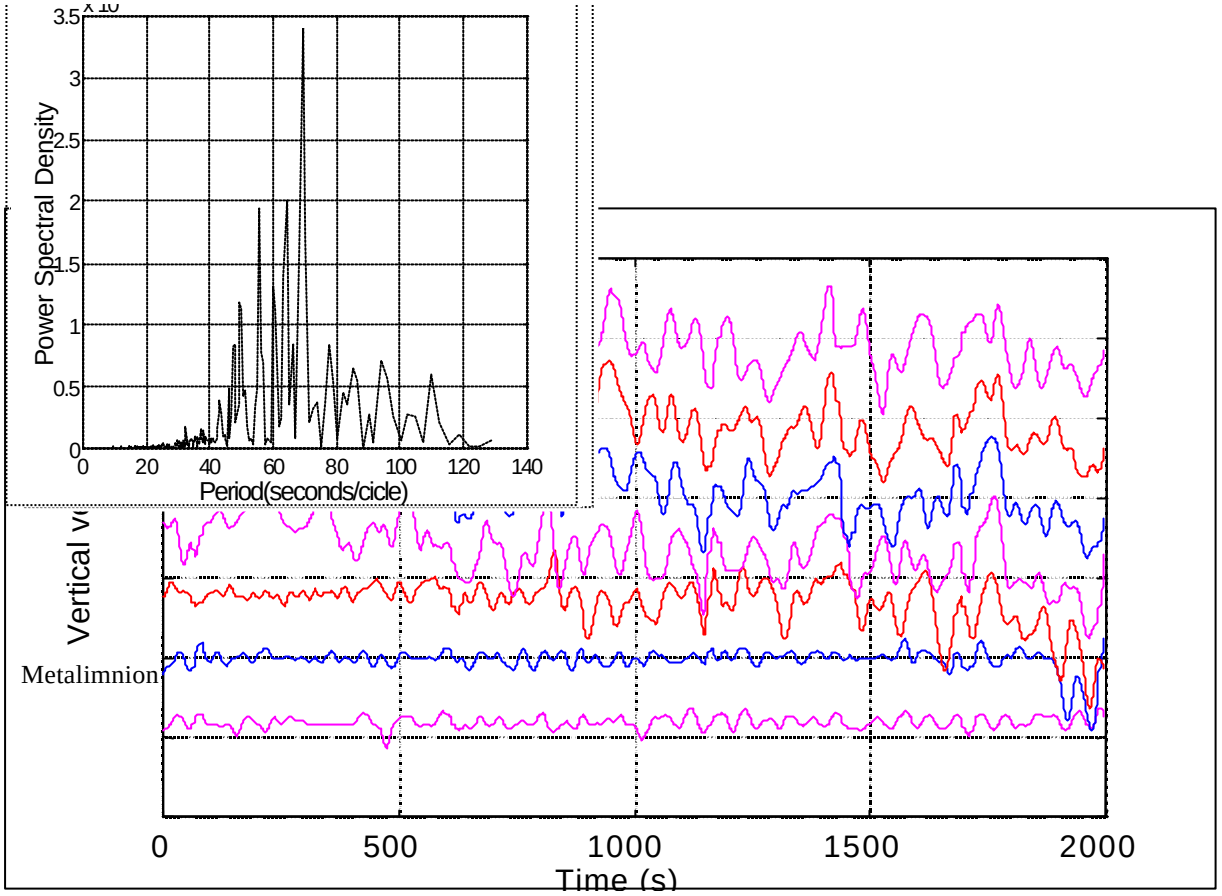

Figure 15 Eulerian vertical velocity component vs time at different depths as obtained from camera A.

The higher frequencies are reflected back up to the mixed layer and only the low frequencies ω_i, for which $\omega_i<N$ (where N is the buoyancy frequency of the density jump i.e. the natural frequency of a vertical displaced particle), can continue to propagate vertically. ω_i must satisfy the dispersion equation (Stull, 1976):

$$\frac{w_i^2}{N^2} = \frac{k_H^2}{k_H^2 + m^2} \tag{2}$$

or:

$$w_i = N \cos q \tag{3}$$

where q is the angle between the horizontal and the resultant wave number vector k (whose component are k_H and m over the horizontal and the vertical direction respectively).

Figure 16 Eulerian vertical velocity component vs time at different depths as obtained from camera B (metalimnion).

Figure 17 Power spectral density of vertical velocity component vs period, obtained from camera B (metalimnion).

However, with reference to the internal wave activity it is worth to note that the present experiment cannot be considered in a steady state as the buoyancy frequency profiles substantially evolve over the time. As a result, several energy peaks are present as can be seen in figure 17 in which is represented the power spectral density of vertical velocity component at different periods, with the most important peak corresponding to the higher buoyancy frequency (i.e. the strongest temperature step).

The similarity with the temperature fluctuations is best seen by plotting the power spectral density for the vertical velocity of particles framed by camera B. Once again the spectrum decreases fairly rapid reaching the bandwidth that corresponds to the range of the evolving buoyancy frequencies with the most significant one of $10^{-1,819}$ Hz (around 66 seconds).

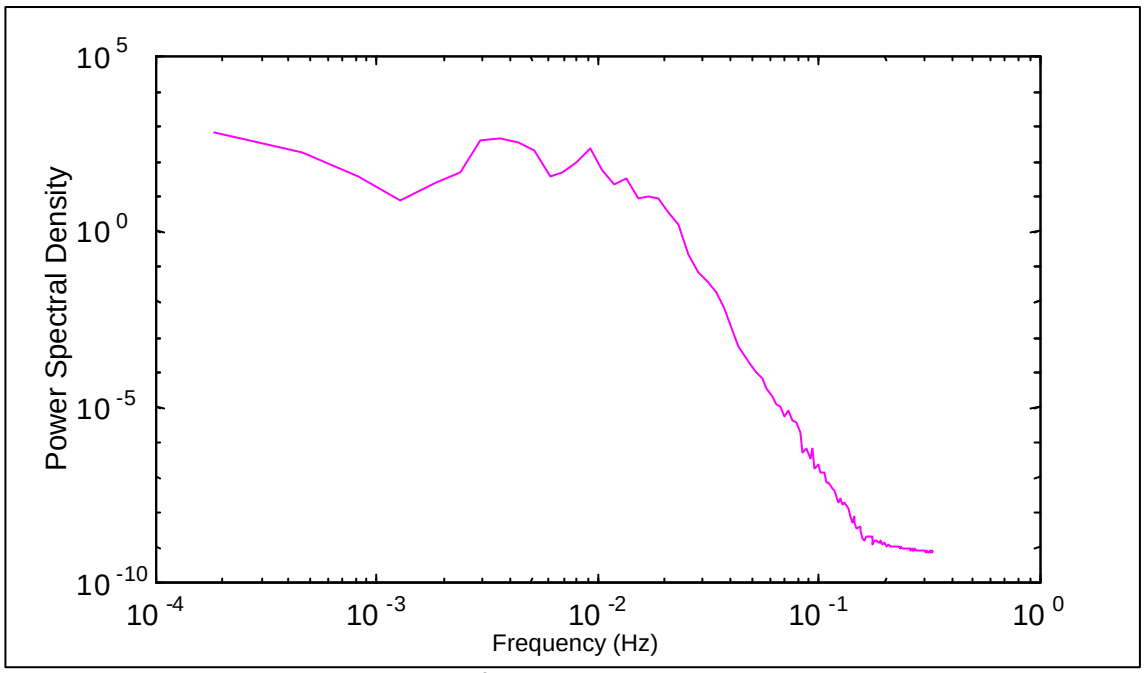

Figure 18 Power spectral density of vertical velocity component obtained by camera

Conclusion

An experiment aimed to analyze the interaction of convective turbulence and the density interface of a stratified lake was carried out. Despite the environmental consequence in terms of nutrients and pollutants flux through the interface this interaction has not a proper analytical description yet. Particularly the properties of the internal wave field are not well understood for the case of penetrative convection. Analysis of image technique are now widely used in laboratory experiments in order to get a detailed picture of the field of motion. The application of PTV allows lagrangian description of particles motion particularly useful in studying dispersion processes, as in the case being. The eulerian field of motion is then inferred by lagrangian information and used to characterize the energetic of the phenomenon both in the mixed layer and in the stratified metalimnion. Another important advantage of PTV is the possibility to storage the information and to analyze it later, when necessary. Penetrative convection is a completely 3D phenomenon which causes most of the particle to leave the thin sheet at a certain depth thus allowing only few of the structures to be fully described by the tracked trajectories in the upper layer. However the motions inside the metalimnion are have smaller scales especially on the horizontal plane allowing the particle to stay on the framed volume for a very long time. The results seem so to confirm the effectiveness of the employed tracking technique to study the internal wave field. Spectral analysis of temperature and velocity signals highlighted the presence of several frequency where energy is concentrated, with the most important one corresponding to the initial strongest temperature jump. An interesting result was the enhanced increase of temperature caused by internal wave in the metalimnion. As the deeper colder fluid is raised up by internal wave oscillation it becomes surrounded by lighter fluid. Without loosing its identity the colder fluid is able to increase its temperature by thermal diffusion acquiring the heat of the hotter fluid. The result is a heat transfer rate much higher than the one due to simple molecular diffusion because of the enhanced temperature difference of the two fluid masses. The same happens to any other substance whose concentration presents a vertical gradient. Together with entrainment this is an important mechanism regulating the flux of nutrients and pollutants through the interface. The present results could be improved by using stereoscopic PTV technique, allowing to track also the velocity component normal to the shot plane of the single camera in order to follow the particle in the ML for time definitively bigger than the time scale of motion.

Bibliography

Andreasson, P., 1992 Energy conversions in turbulent wind-induced countercurrent flow. *J. Hyd. Res.*, **30**: 783-800.

Cenedese, A and G. Mancini. 1999 Application of Particle Tracking Velocimetry to the study of Penetrative Convection in Proc.of the 8th International Conference on Laser Anemometry, Advanced and Applications Rome September 6-8, 1999: 381-389.

Dahm, W. J., Scheil, C. M., Tryggvason, G. 1989 Dynamics of vortex interaction with a density interface. *Journal of Fluid Mechanics,* **205**: 1-43.

Denman, K.L., Gargett, A. E. 1995 Biological-physical interaction in the upper ocean: The role of vertical and small scale transport processes. *Annual Review of Fluid Mechanics*, **27**: 225-255.

Hannoun, I. A., Fernando, J. S., and List, E. J. 1988 Turbulence structure near a sharp density interface. *Journal of Fluid Mechanics*, **189**: 189-209.

Ivey, G. N. and J. Imberger, 1989 On the nature of turbolence in a stratified fluid. Part I: The energetics of mixing. *J. Phys. Oceanogr.*, **21**: 650-658.

Linden P. F., 1975, "The deepening of a mixed layer in a stratified fluid", *Journal of Fluid Mechanics*., **71**: 385-405.

Long, R. R. 1978 A theory of mixing in a stably stratified fluid. *Journal of Fluid Mechanics*., **84**: 113-24.

Querzoli, G. 1996 A lagrangian study of particle dispersion in the unstable boundary layer. *Atmospheric Environment*., **30**: 2821-2829

Sherman F. S., J. Imberger J. and Corcos G. M. 1978, "Turbulence and mixing in stratified waters" *Ann. Rev. Fluid Mech.*, **10**: 277-288.

Stevens C. and Imberger J. 1994 Downward propagatine internal waves generated at the base of the surface layer of a stratified fluid. *Geophysical Research Letters*, **21**, 361-364

Stull R.B., 1976 Internal gravity waves generated by penetrative convection *J. Atmos. Sci.*, **33**: 1260-1267.

Weinstock J., 1984, "Effect of gravity waves on turbulence decay in stratified fluids", *J. Fluid Mech*., **140**: 11-26.